Synthetic and Systems Biotechnology 7 (2022) 513–521

Contents lists available at ScienceDirect

Synthetic and Systems Biotechnology

journal homepage: www.keaipublishing.com/en/journals/synthetic-and-systems-biotechnology

Original Research Article

Improved L-phenylglycine synthesis by introducing an engineered cofactor self-sufficient system

Pengchao Wang [a,b], Xiwen Zhang [a], Yucheng Tao [a], Xubing Lv [a], Shengjie Cheng [a], Chengwei Liu [a,b,*]

[a] School of Life Science, Northeast Forestry University, Harbin, 150040, Heilongjiang, PR China
[b] Key Laboratory for Enzymes and Enzyme-like Material Engineering of Heilongjiang, PR China

ARTICLE INFO

Keywords:
L-phenylglycine
Whole-cell biocatalyst
Self-sufficient
Protein scaffold
Hydroxymandelate synthase

ABSTRACT

L-phenylglycine (L-phg) is a valuable non-proteinogenic amino acid used as a precursor to β-lactam antibiotics, antitumor agent taxol and many other pharmaceuticals. L-phg synthesis through microbial bioconversion allows for high enantioselectivity and sustainable production, which will be of great commercial and environmental value compared with organic synthesis methods. In this work, an L-phg synthesis pathway was built in *Escherichia coli* resulting in 0.23 mM L-phg production from 10 mM L-phenylalanine. Then, new hydroxymandelate synthases and hydroxymandelate oxidases were applied in the L-phg synthesis leading to a 5-fold increase in L-phg production. To address 2-oxoglutarate, NH_4^+, and NADH shortage, a cofactor self-sufficient system was introduced, which converted by-product L-glutamate and NAD^+ to these three cofactors simultaneously. In this way, L-phg increased 2.5-fold to 2.82 mM. Additionally, in order to reduce the loss of these three cofactors, a protein scaffold between synthesis pathway and cofactor regeneration modular was built, which further improved the L-phg production to 3.72 mM with a yield of 0.34 g/g L-phe. This work illustrated a strategy applying for whole-cell biocatalyst converting amino acid to its value-added chiral amine in a cofactor self-sufficient manner.

1. Background

To date, more than 900 naturally occurring amino acids have been identified [1]. Most of them are non-proteinogenic chiral amino acid, which are becoming increasingly important to modern drug discovery. These amino acids are used as antimetabolites of common amino acids and serve as effective inhibitors for a series of metabolic targets [2]. It is estimated that optically active amine including amino acids make up approximately 40% of all chiral intermediates involved in the production of active pharmaceutical ingredients [3].

L-phenylglycine (L-phg) is a non-proteinogenic amino acid, which is used as the building block of virginiamycin S, pristinamycin I, penicillin, and antitumor compound taxol [4–6]. Currently, the synthesis of L-phg is based on petrochemical feedstocks. The process uses environmentally harmful organic solvents and poisonous reagents and the low enantioselectivity which does not meet the demands of environmental safety and green chemistry [7]. A fermentative process to produce chiral amino acids is preferable because of its high enantioselectivity, sustainable raw material, and relatively reduced environmental detriments. Previous studies have reported overproduction of L-phg based on glucose, L-phenylalanine (L-phe), and other substrates [2,8–10].

There are two natural biosynthetic pathways of L-phg production from phenylpyruvate (PPA). One was discovered in *Streptomyces pristinaespiralis* [11]. In this pathway, PPA is converted to phenylacetyl-CoA by the PglB/C pyruvate dehydrogenase-like complex. In the next step, Phenylacetyl-CoA is oxidized to benzoylformyl-CoA by PglA. CoA residue from benzoylformyl-CoA is released by the thioesterase PglD, yielding phenylglyoxylate (benzoylformate, PG). With L-phe as an amino donor, PglE further converts PG to L-phg (Fig. 1a the pathway in blue background). This natural L-phg operon is expressed in different actinomycetal host strains by genetic engineering and fermentation optimization, with L-phg reaching 1.6 μg/L in 96 h^2. The other pathway is characterized in *Streptomyces coelicolor* and *Amycolatopsis orientalis*. PPA is converted to L-mandelate (L-MA) by 4-hydroxymandelate

Peer review under responsibility of KeAi Communications Co., Ltd.
* Corresponding author. No. 26 Hexing Road, Harbin, 150000, China.
E-mail address: liuchw@nefu.edu.cn (C. Liu).

https://doi.org/10.1016/j.synbio.2021.12.008
Received 16 August 2021; Received in revised form 18 November 2021; Accepted 16 December 2021

synthase (HmaS). L-MA is then converted to PG by 4-hydroxymandelate oxidase (Hmo) [9,12,13]. Finally, the PG is further converted to L-phg or D-phg by 4-hydroxyphenylglyoxylate aminotransferase (HpgAT) or D-phenylglycine aminotransferase (DAT) with L-phe and L-glutamate (L-glu) as the amino donor, respectively (Fig. 1a pathway in red background) [8,14]. In some research, this pathway has been employed to produce D/L-phg in *E. coli*. However, the poor activity of HmaS and Hmo (<11 mU/mg) [9] and the low expression level of these heterologous enzymes in *E. coli* hinder the L-phg production. The L-phg production was 51.6 mg/g dry cell weight and 91.4 mg/L from glucose or L-phenylalanine as subtrate [6,8].

In the meantime, researchers have developed other biological routes for L-phg synthesis. In one, racemic mandelate is used as the substrate. Mandelate racemase (MR) coupled with D-mandelate dehydrogenase (MD) catalyzes the substrate to produce PG, which is converted to L- or D-phg by HpgAT or DAT (Fig. 1b) [10,15,16]. A recent example for L-phg production used leucine dehydrogenase (LeuDH) to catalyze the conversion of PG to L-phg using NADH and NH_4^+ as cofactor. To get sufficient redox supply, formate dehydrogenase was co-expressed, which regenerated NADH by oxidizing formate to CO_2. By co-expressing of FDH with LeuDH, 60.2 g/L L-phg was obtained with 99% yield, which showed a satisfactory productivity and enantioselectivity towards L-phg (Fig. 1c) [7,17]. These examples showed us the application of transferases and amine dehydrogenases in prochiral ketones reduction for chiral amines synthesis. In this process, the sufficient supply of amine donor and redox were important for successful engineering.

The cascade (or "domino") one-pot reaction is successfully performed by sequential or simultaneous reactions to produce chiral alcohols, amines, as well as amino acids [16]. Cascading reaction often involves the participation of oxidoreductase, together with generation or consumption of NAD(P)H, which can lead to a stoichiometric redox imbalance. In many cases, formate dehydrogenase and glucose dehydrogenase are used to recycle NAD (P) H by oxidation of sacrificial substrates [18–20]. In our previous work, a synthesis pathway from L-phe to 2-phenylethanol (2-PE) was coupled with glutamate dehydrogenase (GDH) as a cofactor regeneration module [21]. Using this module, no external cofactor or redox source was required as GDH utilized the by-product L-glu and NAD(P)$^+$ to simultaneously synthesize the co-substrates 2-oxoglutarate (2-OG) and NAD(P)H (Fig. 2a) [21]. Theoretically, this redox self-sufficient system is also feasible for any amino acid to its value-added amine derivatives, if this bioconversion process meets the following two conditions, (a) the substrate amino acid deamination was catalyzed by a transaminase with 2-OG as amino group acceptor, (b) the product amine derivatives use NAD(P)H and NH_4^+ as cofactor for its amination. We suppose that L-phg synthesis from L-phe is suitable for this system. The TyrB catalyzes L-phe and 2-OG to PPA and L-glu, then PPA is converted to PG following the pathway in *S. coelicolor* and *A. orientalis*. At last, LeuDH convert PG to L-phg with the utilization of NADH and NH_4^+. By introducing the cofactor regeneration module, by-product L-glu could be converted to 2-OG, NADH and NH_4^+, which are all needed redox and co-substrate in L-phg synthesis. In this manner, no redox needs to be added, even NH_4^+ in this system stoichiometric balanced (Fig. 2b).

In this study, we exemplified a self-sufficient biotransformation system from amino acid L-phe to its value-added chiral amine derivatives L-phg. Firstly, an L-phg pathway was built in *E. coli* BW25113. New HmaS and Hmo were expressed to improve the synthesis efficiency. Then, the cofactor regeneration module was introduced to maintain redox balance and amino group recycling. Finally, a protein scaffold was used to enhance the connection between the synthetic pathway and cofactor regeneration module to obtain better L-phg production.

2. Results

2.1. Construction of L-Phg biosynthetic pathway in E. coli

A heterologous L-phg pathway was constructed by co-overexpressing the aromatic transaminase ($tyrB_{Ec}$) from *E.coli*, hydroxymandelate synthase ($hmaS_{Sc}$) and hydroxymandelate oxidase (hmo_{Sc}) from *S. coelicolor*, and a codon-optimized leucine dehydrogenase ($leuDH_{Bc}^{opt}$) from *Bacillus clausii* (Fig. 2b). Based on our previous research, the enzyme activity of $TyrB_{Ec}$ and $LeuDH_{Bc}$ were much higher than $HmaS_{Sc}$ and Hmo_{Sc} [9,17]. Therefore, these genes were divided into two operons, $hmaS_{Sc}$-hmo_{Sc} were gibson assembled into high copy plasmid pYB1s, and $leuDH_{Bc}^{opt}$--$tyrB_{Ec}$ were gibson assembled into a medium copy plasmid pRB1a. These

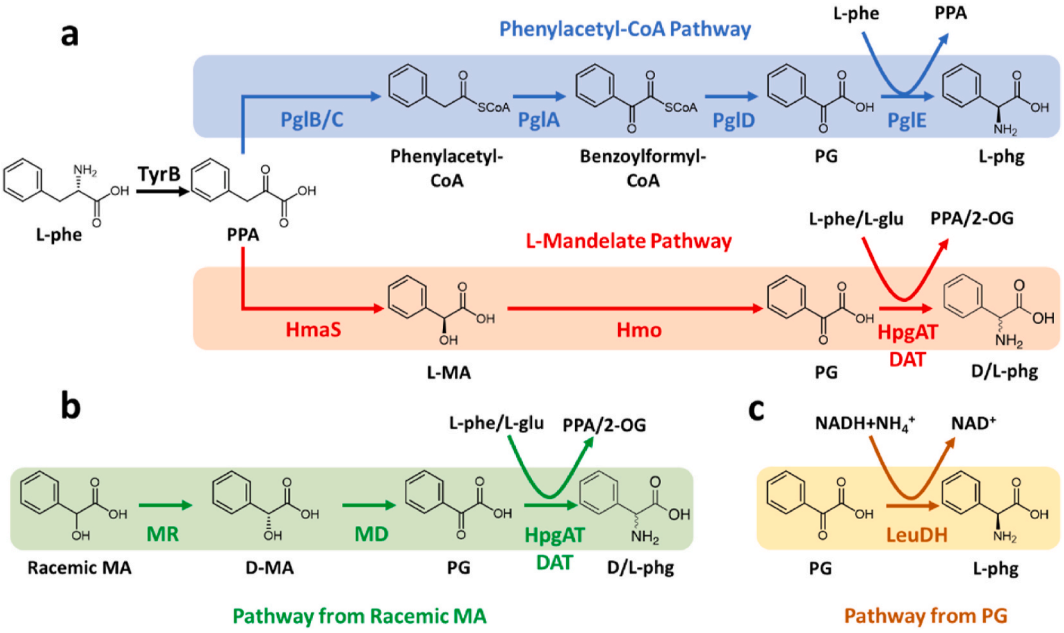

Fig. 1. Current L-phg synthesis pathways based on different substrates. (a) Summary of natural L-phg synthesis pathway from PPA as substrate. The pathway in bule or red background was the L-phg synthesis pathway identified from Streptomyces pristinaespiralis or Streptomyces coelicolor and Amycolatopsis orientalis respectively. (b) L-phg synthesis pathway from racemic MA. (c) L-phg synthesis pathway from PG.

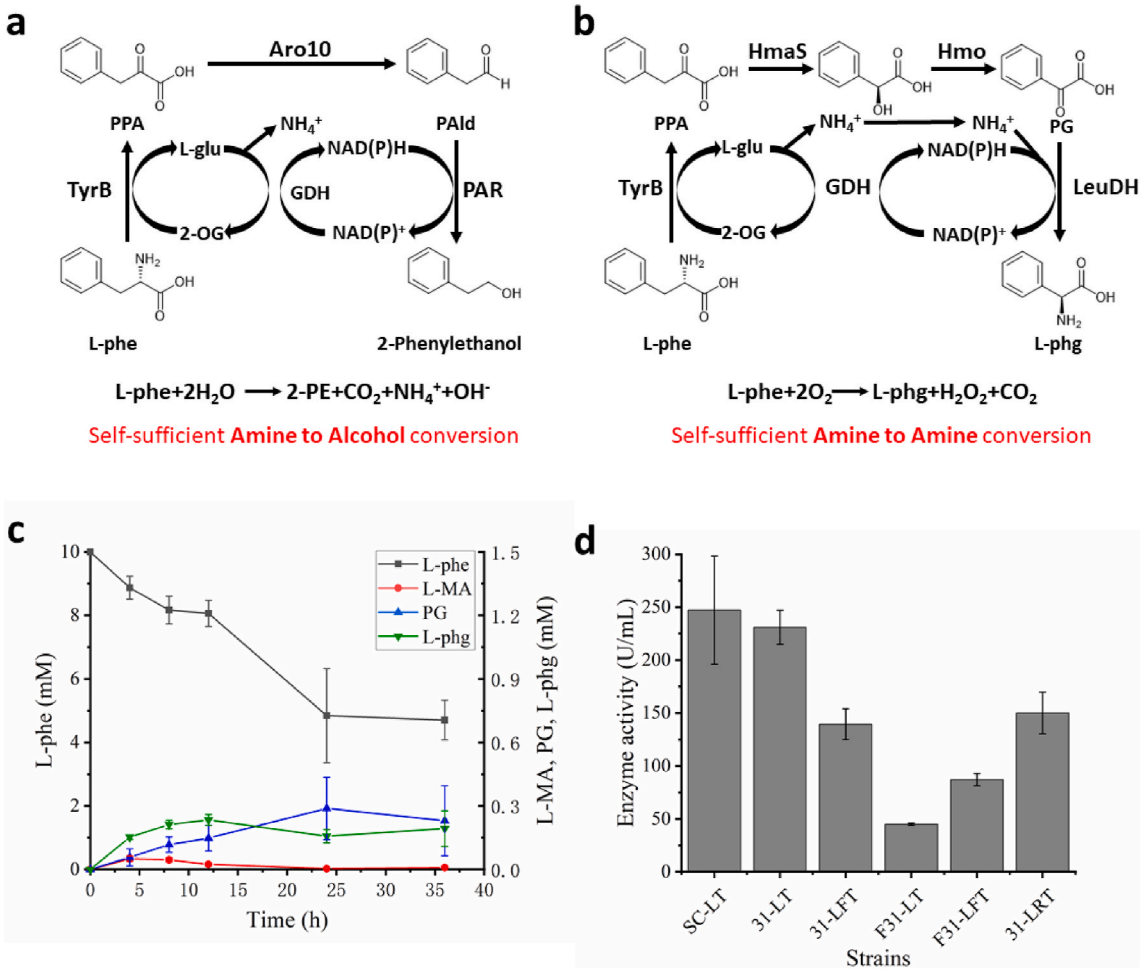

Fig. 2. Design of self-sufficient module for L-phg production (a) Self-sufficient biocatalyst design for conversion of amino acids to the corresponding alcohol. In this system, by-products L-glu and NAD(P)+ were converted to co-substrates 2-OG, NAD(P)H simultaneously, the only waste was NH4+ produced by GDH. (b) Self-sufficient biocatalyst design for conversion of amino acid L-phe to its value-added chiral amine derivatives L-phg. By introducing cofactor regeneration modular, co-substrates are all balanced. (c) Time curve of L-phe, L-MA, PG, and L-phg of strain SC-LT. (d) LeuDH activities of different strains. Cells were harvested and resuspended to an optical density at 600 nm of 30. LeuDH activity in the cell lysates was measured by monitoring the consumption of NADH.

two plasmids have the same arabinose-inducible promoter, but the origin and selective marker of pYB1s were P15A and streptomycin while the pRB1a were R6K and ampicillin. The resulting *E. coli* BW25113 harboring pYB1s-$hmaS_{Sc}$-hmo_{Sc} and pRB1a-$leuDH_{Bc}{}^{opt}$-$tyrB_{Ec}$ (designated SC-LT, protein expression results showed in Fig. S2c) was used as the whole-cell biocatalyst.

After a 12-h biotransformation, 0.23 mM (35.3 mg/L) L-phg was obtained from 10 mM L-phe. As Fig. 2c shows, only 2 mM L-phe was catabolized in the first 12 h. Over time, the substrate L-phe decreased slowly, while the final product, L-phg did not further accumulate. And the intermediates L-MA and PG kept in a low concentration. These results indicated that L-phg production was hampered by the insufficiency of enzymes in this pathway. TyrB was a protein from *E. coli*, SDS-PAGE showed that it had a very high soluble expression (Fig. S1). Previous study showed that the specific activity of TyrB was 170 μmol/min/mg towards L-phe [22]. In our previous study on 2-PE synthesis, TyrB could catalyze the conversion of 20–40 mM L-phe to PPA in 12 h [21]. At the same time, the residual LeuDH enzyme activity after 12 h of bioconversion was measured. As shown in Fig. 2d, the residual LeuDH activity of SC-LT was 247.3 U/mL. Based on SDS-PAGE, there were solubility problems in HmaS and Hmo expression (Fig. S1). Given the fact that the enzymes activity of HmaS and Hmo were low [6], we supposed that the insufficiency of HmaS and Hmo were the bottlenecks in this L-phg biosynthesis pathway.

2.2. Optimization L-phg production using different combinations of HmaS and Hmo

In previous studies, HmaS and Hmo from *S. coelicolor* and *A. orientalis* were expressed in *E.coli* for phenylglycine synthesis. The activity of $HmaS_{Sc}$ and Hmo_{Sc} were 2.2 mU/mg and 4.7 mU/mg to PPA and L-MA respectively [9], which may be improved by screening new HmaS and Hmo. Protein sequences annotated as HmaS in Kyoto Encyclopedia of Genes and Genomes were downloaded and used for phylogenetic analysis. As Fig. 3a showed, HmaS could be divided into six main branches. We selected six HmaS from each branch, including previously reported HmaS from *S. coelicolor* and *A. orientalis*. They are HmaS from *S. coelicolor*, *A. orientalis*, *Actinosynnema mirum*, *Micromonospora tulbaghiae*, *Myxococcus stipitatus* and *Herpetosiphon aurantiacus*. The genes encoding six HmaS were codon optimized based on *E. coli* preference, namely $hmaS_{Sc}{}^{opt}$, $hmaS_{Ao}{}^{opt}$, $hmaS_{Am}{}^{opt}$, $hmaS_{Mt}{}^{opt}$, $hmaS_{Ms}{}^{opt}$, $hmaS_{Ha}{}^{opt}$ (numbered as *hmaS1-hmaS6*). According to references, *S. coelicolor*, *A. orientalis*, *A. mirum, M. tulbaghiae*, were widely used host for β-lactam antibiotics and glycopeptide antibiotics fermentation indicating that they may have a more active L-phg synthesis pathway [23–26]. Therefore, the Hmo encoding genes from these four organisms were synthesized too ($hmo_{Sc}{}^{opt}$, $hmo_{Ao}{}^{opt}$, $hmo_{Am}{}^{opt}$, $hmo_{Mt}{}^{opt}$ numbered as *hmo1-hmo4*). The expression level of each *hmaS1-6* and *hmo1-4* were analyzed by SDS-PAGE (Showed in Fig. S2 a and b). *hmaS1-6* and *hmo1-4*

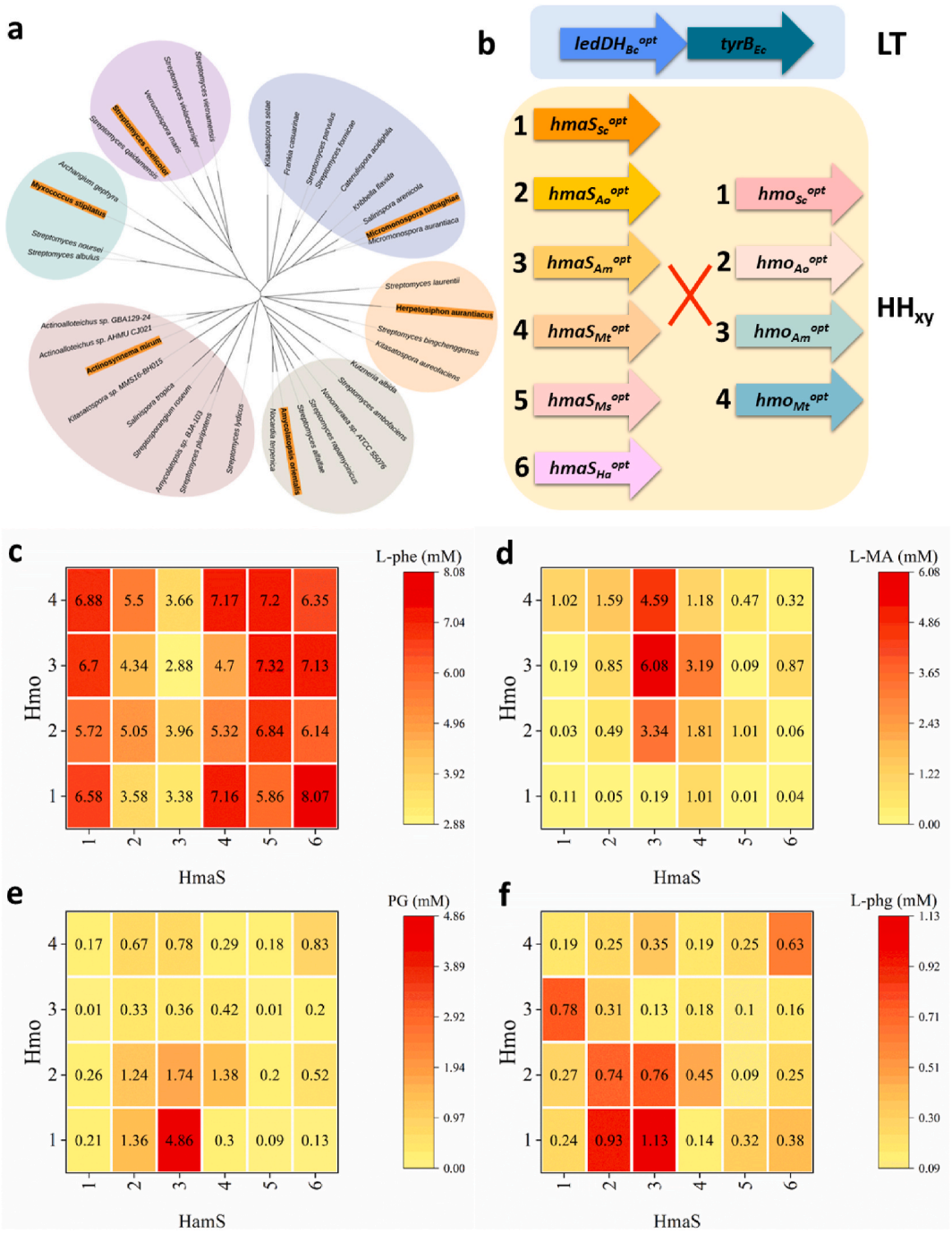

Fig. 3. L-phg production from L-phe by whole-cell bioconversion using different recombinant E. coli strains. (a) The phylogenetic tree analysis of HmaS. HmaSs were chosen from each phylogenetic branches for L-phg production. (b) Operons built in this study, LT represents the plasmid harbouring operon leuDHBcopt-tyrBEc. The HHxy represents the plasmid harbouring operon hmaSx-hmoy, x (1–6) represents different hmaS, y (1–6) represents different hmo. HHxy coexpressed with LT form 24 combinations. (c–e) The concentration of metabolites L-phe, MA, PG, L-phg of these 24 combinations. The abscissa axis represents the hmaS used and the ordinate axis represents the hmo used. The concentration of the each metabolite was visualized by a heat map.

were gibson assembled to each other under a pBAD promoter in expression vector pYB1s resulting plasmids HHxy (the x denotes the *hmaS* and y denotes the *hmo* assembled in plasmid, for example HH23 represents the plasmid expressing *hmaS2* and *hmo3*). The HHxy together with pRB1a-*leuDH*$_{Bc}^{opt}$-*tyrB*$_{Ec}$ formed 24 different combination strains (i.e., HH11-LT to HH64-LT, Fig. 3b) (HH11-LT and HH31-LT protein expression results showed in Fig. S2c).

After 12-h biotransformation, the substrate distribution of 24 strains was measured. As heatmap showed in Fig. 3c–f. Significant differences in L-phe utilization were observed according to different *hmaS-hmo* combinations. In most *hmaS-hmo* combinations, only 20–50% of L-phe was used (Fig. 3c), except that *hmaS3* utilized up to 60%–71% of the L-phe and produced significantly higher intermediate L-MA, PG (Fig. 3d and e). Strain HH33-LT produced 6.1 mM L-MA, accounting for 85.4% of the L-phe utilized. Strain HH31-LT produced 4.9 mM PG, which was 73.4% of L-phe utilized.

Different intermediates distributions were observed when *hmaS3* was accompanied with different *hmo* too. When *hmo2*, *hmo3* or *hmo4* was coupled with *hmaS3*, 3.3–6.1 mM L-MA was accumulated (Fig. 3d) and only a small amount of L-MA (0.5–2.5 mM) was subsequently

converted to PG and L-phg (Fig. 3e and f). In contrast, *hmo1* converted almost all L-MA to the subsequent steps (Fig. 3d). These differences suggested that *hmo1* had the best catalytic performance among *hmo1-4*. Among 24 *hmaS-hmo* combinations, *hmaS3-hmo1* was the most efficient. This strain produced 1.13 mM (172.9 mg/L) L-phg (Fig. 3f), which was 5-times higher than that of SC-LT.

Another result should be noticed that PG accumulation in strain HH31-LT was markedly higher than other strains (4.86 mM, Fig. 3e). The reason for this result could be the low catalytic activity of $LeuDH_{Bc}$ or inadequate cofactor NADH or NH_4^+. For further analysis of the main cause, the $LeuDH_{Bc}$ activity in strain 31-LT was tested after a 12-h biotransformation. The activity was 231 U/L (Fig. 2d). This result indicated that under ideal conditions, $LeuDH_{Bc}$ could catalyze 13.9 mM PG to L-phg per hour. Thus, cofactor NADH or NH_4^+ shortage was considered as the major bottleneck in HH31-LT biotransformation process, rather than LeuDH activity.

2.3. Introduction of a NADH regeneration module for higher L-phg production

The $LeuDH_{Bc}$ activity was proved to be not the main problem in HH31-LT, leading to the shortage of cofactor NADH or NH_4^+ might block L-phg synthesis from PG. An NAD^+-dependent formate dehydrogenase (FDH) from *Candida boidinii* was used to enhance the NADH supply. FDH is widely used as an NADH regeneration module as it catalyzes the oxidation of formate to simultaneously produce CO_2 and NADH [27,28]. $fdh_{Cb}{}^{opt}$ was codon optimized and inserted into either plasmid containing the $leuDH_{Bc}{}^{opt}$-$tyrB_{Ec}$ operon or *hmaS3-hmo1* operon and resulted in plasmid LFT and F31 (Fig. 4a). Strains HH31-LFT, F31-LT, and F31-LFT were used for L-phg production. When $fdh_{Cb}{}^{opt}$ was overexpressed, 20 mM sodium formate and 50 mM NH_4Cl were added for efficient supply of NADH and NH_4^+.

Integrating $fdh_{Cb}{}^{opt}$ to $leuDH_{Bc}{}^{opt}$-$tyrB_{Ec}$ operon or hmaS3-hmo1 operon made a big difference in L-phe utilization. When $fdh_{Cb}{}^{opt}$ coexpressed with $leuDH_{Bc}{}^{opt}$-$tyrB_{Ec}$ (HH31-LFT) 2.6 mM L-phe left (Fig. 4b). When $fdh_{Cb}{}^{opt}$ was coexpressed with *hmaS3-hmo1* in strain F31-LT, a majority of L-phe (7.3 mM) remained unused. Strain F31-LFT which harboring two copies of $fdh_{Cb}{}^{opt}$ had similar metabolite distributions with F31-LT. We believed the expression of $fdh_{Cb}{}^{opt}$ in *hmaS3-hmo1* operon took up the resources originally used for *hmaS3-hmo1* expression, which turned down the L-phg synthetic pathway. Therefore, strains F31-LT and F31-LFT utilized significantly lower L-phe than HH31-LT and HH31-LFT (Fig. 4b). When operon $leuDH_{Bc}{}^{opt}$-$fdh_{Cb}{}^{opt}$-$tyrB_{Ec}$ was overexpressed (HH31-LFT), L-phg production reached 2.38 mM, which was 2.1-times that of the HH31-LT. At the same time, PG decreased 11% due to the increased NADH supply (Fig. 4b).

2.4. Construction of a self-sufficient module for L-phg production

Co-expression of $fdh_{Cb}{}^{opt}$ with the L-phg synthesis pathway increased L-phg production, indicating that insufficient NADH supply was the major reason for PG accumulation. We noticed that, there were two co-substrates that were also essential for L-phg production. One was 2-OG, which acts as the amino acceptor in L-phe deamination. The other was NH_4^+, which is necessary for the amination of L-phg. Recently, we developed and successfully applied a cofactor self-sufficient system for 2-PE production, which could regenerate co-substrate (2-OG, NH_4^+) and redox equivalents (NADH) simultaneously. This strategy eliminated the need for external co-substrate or redox source. (Fig. 2a). We believed that introducing the cofactor regeneration module would further improve the L-phg production.

An NADH-dependent GDH encoded by $rocG_{Bs}$ from *B. subtilis* was inserted into $leuDH_{Bc}{}^{opt}$-$tyrB_{Ec}$ operon (Fig. 4a, designated as LRT) and coexpressed with HH31 [29] (protein expression results showed in Fig. S2c). The strain HH31-LRT used 7.8 mM substrate, 18% higher compared with strain had no $rocG_{Bs}$ (Fig. 4c). This result indicated that more 2-OG was regenerated by $rocG_{Bs}$. In the meantime, the concentrations of L-MA and PG increased from 0.20 to 4.86 mM to 0.68 and

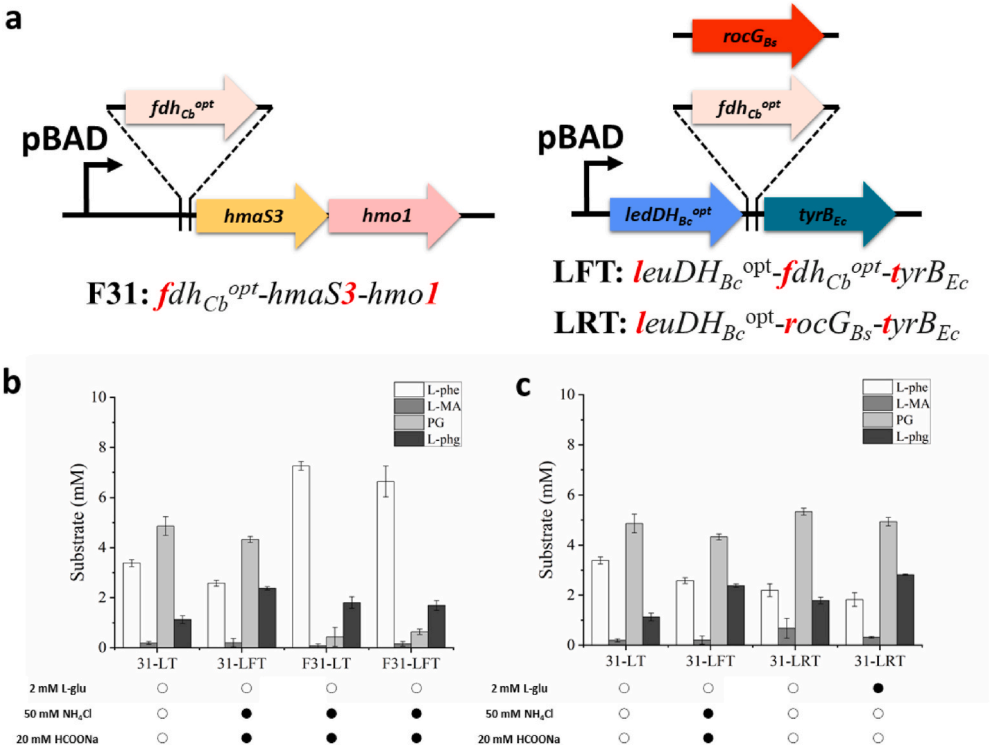

Fig. 4. L-phg production using different NADH regeneration strategies. (a) The plamids carrying fdhCbopt and rocGBs. (b) Production of L-phg by strains with or without FDH. When FDH was coexpressed, 50 mM NH4Cl and 20 mM HCOONa were added simultaneously. (c) Production of L-phg by strains with FDH or GDH. L-glu (2 mM) was added to enhance the cofactor regeneration by GDH.

5.33 mM, respectively, and L-phg production increased by 58% from 1.13 to 1.79 mM compared with strain had no $rocG_{Bs}$ (Fig. 4b). Furthermore, L-glu was proved to have a positive effect on cofactor regeneration in our previous work [21]. Therefore, 2 mM L-glu was used to enhance cofactor regeneration. The addition of L-glu accelerated the utilization of L-phe and PG amination to L-phg. L-phg production increased dramatically from 1.79 mM to 2.82 mM, which was 12.3-times higher than that of the original strain, SC-LT (Fig. 4c).

Although the cofactor regeneration system improved the production of L-phg, accumulation of 4.93 mM PG remained. LeuDH activity was measured to determine whether enzyme activity or NADH and NH_4^+ caused insufficient conversion of PG to L-phg. When co-expressed with $rocG_{Bs}$ or fdh_{Cb}^{opt}, LeuDH activities were 150.1 and 139.5 U/mL, respectively (Fig. 3b). The enzyme assay showed that the activity of LeuDH was sufficient to convert more PG to L-phg. Thus, NADH and NH_4^+ supply was further enhanced.

2.5. Spatial organization of cofactor self-sufficient module and LeuDH

Synthetic scaffolds have been widely used to enhance product synthesis by avoiding the intermediate loss that occurs by competing pathways [30,31]. In this study, the cofactor regeneration module and LeuDH were spatially organized by a synthetic protein scaffold to form a substrate channel for NADH and NH_4^+ which conserved more 2-OG and NH_4^+ for L-phg production rather than used by cell central metabolism (Fig. 5b). SH_3 and slig protein-protein interaction domains were fused to the C-terminus of $rocG_{Bs}$ and $leuDH_{Bc}^{opt}$ by a flexible linker (GGGGS) [32]. By altering the number of slig, one to three $rocG_{Bs}$ conjoined with one $leuDH_{Bc}^{opt}$ to adequately supply NADH and NH_4^+. The strains with recombinant plasmids were designated slig-1, slig-2, and slig-3 (Fig. 5b).

The scaffold SH_3-slig closely colocalized $leuDH_{Bc}^{opt}$ and $rocG_{Bs}$. This prevented the diffusion of NADH and NH_4^+, and facilitated the conversion of PG to L-phg. This strategy resulted in an increase of L-phg to 3.28, 3.72, and 3.01 mM in slig-1, slig-2, and slig-3, respectively. Compared with 31-LRT, slig-2 produced more than 2-fold of L-phg. The molar yield of L-phg reached 37.2%. The accumulation of PG decreased from 5.3 mM to approximately 4 mM, demonstrating that spatial organization could be an effective method to improve target compound production by reducing the loss of intermediate metabolites.

3. Discussion

L-phg is an important building block of antibiotics [2,33], antitumor drug taxol [34], drugs used to treat Alzheimer's and many other diseases [35,36]. Many progresses have been made on synthesis of L-phg in a biological way [8,10,17]. In this study, we built a L-phg synthesis pathway in *E. coli*. However, only a small amount of L-phe was utilized to synthesis L-phg. As study showed that enzyme activities of HmaS and Hmo from *S. coelicolor* were 0.501 and 1.822 U/mg[6]. At the same time, the solubility of these two enzymes in *E. coli* were low. Thus, HmaS and Hmo was considered as the major bottleneck for L-phg production.

To address this problem, new HmaS and Hmo from different organisms were introduced into L-phg synthesis. 6 HmaS and 4 Hmo were chosen and each HmaS were co-expressed with every Hmo. After enumerating all the combinations of HmaS and Hmo, $HmaS_{Am}$ from *A. mirum* was found to catalyze the most amount of L-phe to L-MA and following intermediates. *A. mirum* produces a variety of biologically active compounds including ansamitocins [37], β-lactam antibiotics validoxylamine A [38] and nocardicin A [39]. The pentapeptide precursor of Nocardicin A has 4-hydroxy-L-phenylglycine at position 1, 3, and 5[40]. Which indicating *A. mirum* may have an active L-phg synthesis pathway. Recently, HmaS from another nocardicin producer, *N. uniformis*, was utilized in *S. cerevisiae* for MA and HMA production which led to a 42% and 90% increase in HMA and MA production [41]. These results indicate that there may be more efficient HmaS and Hmo from other nocardicin producers. L-phg biomanufacturing maybe benefit by further screen new HmaS and Hmo in these strains.

Although more than 6 mM L-phe was converted to PG in HH31-LT, only 1.1 mM L-phg was obtained. The reason for this result could be the low LeuDH activity or shortage of NADH and NH_4^+. The LeuDH activity assay showed it was adequate. Therefore, the limited cofactor and NH_4^+ were believed to be the major bottlenecks. Two approaches were applied to address these bottlenecks. One was coupling an NADH regeneration enzyme FDH with L-phg pathway. The FDH could oxidize sodium formate and regenerate NADH simultaneously.This strategy has been successfully applied in L-tert leucine, ethanol, phenyllactic acid synthesis [42–45]. As a result, more than 2-fold L-phg was obtained, indicating that NADH and NH_4^+ were the major problems in L-phg synthesis.

The other strategy was inspired by our previous work (Fig. 2a), an Ehrlich pathway was established in *E. coli* to produce 2-PE from L-phe. By co-expressing GDH, the L-glu and NAD(P)$^+$ byproducts were able to simultaneously regenerate to 2-OG and NADPH, which lead to 3.8-fold 2-PE increased [21]. In this study, we adopted this strategy to an amino acid to its valued-added chiral amine derivatives. Similar to 2-PE biosynthesis, 2-OG and NAD(P)H were essential in L-phg, while NH_4^+ was also necessary. Therefore, the NH_4^+ generated by GDH was reused, and no waste accumulated in this conversion (Fig. 2b). Thus, a self-sufficient cofactor system based on a bridging mechanism was developed to simultaneously rebalance the co-substrate and redox equivalents, so that no external cofactor or redox source was required. Compared with FDH co-expression approach, L-phg production increased by 20% and no additional sodium formate and NH_4Cl were needed, which was a big advantage.

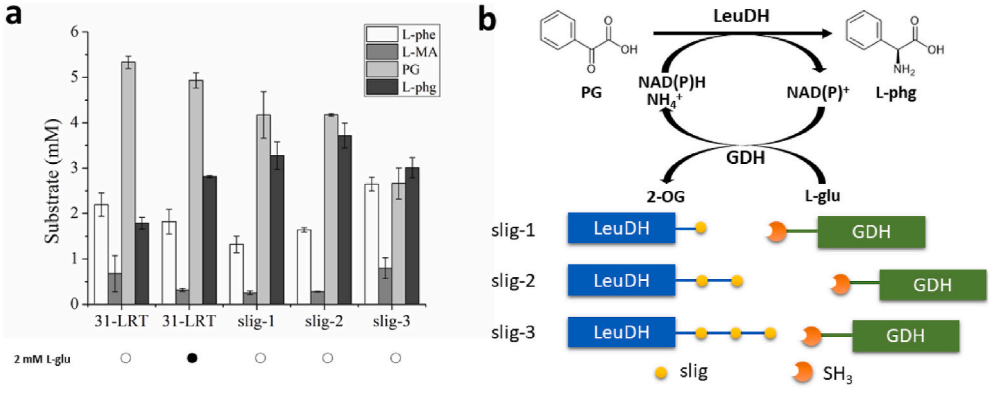

Fig. 5. L-phg production by spatial colocalization of LeuDH and GDH. (a) Metabolite distribution of strains with different ratios of LeuDH to GDH. (b) Schematic diagram of the spatial colocalization of LeuDH and GDH. By altering the number of slig in the C-terminus of LeuDH, different numbers of GDH colocalized with LeuDH, leading to different biocatalytic performance.

Unlike in 2-PE production, when the cofactor regeneration module was applied in L-phg production, we noticed an accumulation of intermediate PG. Even though we designed a stoichiometric balanced reaction, the accumulation of intermediate reminded us that the cofactor regeneration module and the synthetic pathway should function at the same pace. In this way, the regenerated cofactor and redox regenerated could be used by L-phg synthesis rather than used by competing reactions. In L-phg synthesis, cofactor regeneration was faster than the synthetic pathway, leading to the faster regeneration of 2-OG and NADH than the synthetic pathway. The 2-OG was used to convert L-phe to PPA and L-glu. L-glu recycled and produce 2-OG and NADH, which further accelerate the conversion of L-phe to PPA (Fig. 2b). In this situation, NADH in the engineered bacteria did not wait until PG generated, but catabolized by other competing reactions instead. Therefore, when PG generated, there were not enough NADH. Compared with HH31-LT, HH31-LRT produced 2.5 folds L-phg, and PG decrease 8%. The problem of PG accumulation was not totally solved.

To retain more NADH, an orthogonal interaction pair slig-SH_3 was applied in order to colocalize LeuDH and GDH. This protein scaffold strategy was first used for mevalonate biosynthesis. By altering the stoichiometry of the SH3, PDZ, and GBD domains, three mevalonate biosynthetic enzymes were arranged in a designable manner, which lowered the host-expressing burden and increased the production of mevalonate 77-fold [32]. Protein scaffolds have been applied to incorporate sequential enzymes in gamma-aminobutyric acid, polyhydroxybutyrate, and resveratrol production [46–48]. In this work, a scaffold was built between the synthetic pathway and cofactor regeneration module. In this way, cofactor NADH, and co-substrate NH_4^+ generated by GDH could be directly utilized by LeuDH. Thus, L-phg increased by 2.1-fold compared with no scaffold. The final L-phg level reached 3.72 mM (562.5 mg/L), which was the highest L-phg titer from L-phe or glucose.

These results exemplified an application of self-sufficient cofactor regeneration strategy in amino acids to its value-added chiral amine derivatives. Moreover, enzyme colocalization was used between synthesis pathway and cofactor regeneration modular and proved to be an effective way to enhance product formation.

4. Material and methods

4.1. Chemicals and reagents

L-phe, L-glu, sodium formate, NH_4Cl, and Tris base were purchased from Shanghai ShengGong Bio-chemical Co. Ltd. (Shanghai, China). For high-performance liquid chromatography (HPLC) analysis, standards for L-phe, PPA, L-MA, PG, and L-phg were purchased from Sigma-Aldrich (Steinheim, Germany). Restriction endonucleases and DNA polymerase were purchased from New England Biolabs (Ipswich, MA, USA). The ClonExpress MultiS One Step Cloning Kit for Gibson assembly was purchased from Vazyme Biotech Co., Ltd. (Nanjing, China).

4.2. Bacterial strains and culture conditions

All strains and plasmids used in this study are listed in Supplementary Table S1. *E. coli* strains were grown at 37 °C on a shaker at 200 rpm in Luria–Bertani (LB) medium with ampicillin and streptomycin (50 μg/mL) added as required. For protein expression, overnight cultures were inoculated (1% inoculum) into auto-induction ZYM medium [49] and incubated with constant shaking at 30 °C for 16 h.

4.3. Plasmid and strain construction

The genes $hmaS_{sc}{}^{opt}$, $hmaS_{ao}{}^{opt}$, $hmaS_{am}{}^{opt}$, $hmaS_{mt}{}^{opt}$, $hmaS_{ms}{}^{opt}$, $hmaS_{ha}{}^{opt}$, $hmo_{sc}{}^{opt}$, $hmo_{ao}{}^{opt}$, $hmo_{am}{}^{opt}$, $hmo_{mt}{}^{opt}$, $leuDH_{Bc}{}^{opt}$, $fdh_{Cb}{}^{opt}$ (translated protein sequence ID: 3ZGJ_A, WP_016331888.1, ACU38423.1, WP_120569635.1, WP_015349166.1, ABX04531.1, WP_011028840.1, WP_016331889.1, ACU37897.1, WP_120569648.1, WP_000171355.1, and CAA09466.2) were codon-optimized based on the *E. coli* codon preference and synthesized by GenScript (Nanjing, China). The $hmas_{Sc}$ and hmo_{Sc} genes were amplified from genome *Streptomyces coelicolor* A3(2) (GI: 30407153). The other genes for L-phg production, including *tyrB* and *rocG*, were amplified from *E. coli* BW25113 (GI: 749300132) and *Bacillus subtilis* subsp. subtilis str. 168 (Sequence ID: CP053102.1) genomic DNA. String DNA fragments with a 20-base pair (bp) overhang were inserted into pYB1a and pRB1s derivatives using the Gibson assembly method. The primers were designed by CE design (https://crm.vazyme.com/cetool/simple.html). They are listed in Supplementary Table S2.

4.4. Bioconversion conditions

For L-phg bioconversion, cells were collected after 16 h of culture by centrifugation at 8000×*g* for 10 min, washed twice with ice-cold 0.85% NaCl solution, and suspended in 200 μL (optical density at 600 nm = 30) of a reaction mixture containing 10 mM L-phe and 50 mM Tris-HCl buffer (pH = 7.0). L-glu, NH_4Cl, and sodium formate were added as required. The bioconversion reactions were performed at 37 °C with shaking at 200 rpm for 12 h.

4.5. Phylogenetic analysis

Gene sequences were downloaded from KEGG (Entry: K16421). Multiple alignments were obtained using Mega5 ClastalW with default parameter (gap open penalty 10, gap extension penalty 0.1). The Phylogenetic tree was built using the Neighbor-joining method with the Bootstrap option. Finally the editing tool iTOL was used.

4.6. Analytical methods

Cell density was estimated by measuring the OD_{600} (1 OD/L = 0.23 g (dry cell weight)/L). To determine LeuDH enzyme activity assay, 200 μL of cell lysate was added to 2 mL of enzyme reaction mixture containing 25 mM Tris-HCl buffer, 1 mM NH_4Cl, 0.1 mM NADH, and 0.2 mM PG (pH = 7.0). One unit of enzyme activity was defined as the amount of enzyme catalyzing the reduction of 1 μmol NADH/min. The concentrations of L-phe, L-MA, PG, and L-phg were measured by HPLC using the Agilent 1260 series device (Hewlett–Packard, Palo Alto, CA, USA) equipped with an XBridge C-18 3.5 μm column (4.6. × 150 mm; Waters, Milford, MA, USA). The analysis was performed at 30 °C with a mobile phase comprising 10% methanol in 20 mM phosphate buffer (pH = 6.5) at a flow rate of 0.5 mL/min. The analytes were detected at OD_{210}.

CRediT authorship contribution statement

Pengchao Wang: Data curation, Formal analysis, Investigation, Conceptualization, Writing – original draft, Writing – review & editing, Funding acquisition. **Xiwen Zhang:** Data curation, Investigation, Formal analysis, Writing – original draft. **Yucheng Tao:** Data curation, Investigation, Formal analysis. **Xubing Lv:** Data curation, Investigation. **Shengjie Cheng:** Data curation, Investigation. **Chengwei Liu:** Project administration, Resources, Conceptualization, Writing – review & editing, Supervision.

Declaration of competing interest

We declare that we have no financial and personal relationships with other people or organizations that can inappropriately influence our work, there is no professional or other personal interest of any nature or kind in any product, service and/or company that could be construed as influencing the position presented in, or the review of, the manuscript entitled “Improved L-phenylglycine synthesis by introducing an engineered cofactor self-sufficient system”

Acknowledgements

We thank Prof. Tao Yong and Prof. Lin Baixue for valuable advises and vectors used in this research. This work was supported in part by the National Natural Science Foundation of China (Project No. 31900064), as well as the Natural Science Foundation of Heilongjiang Province of China (Project No. LH2019C012). The authors declare that they have no competing interests.

Appendix A. Supplementary data

Supplementary data to this article can be found online at https://doi.org/10.1016/j.synbio.2021.12.008.

Abbreviations

L-phe	L-phenylalanine
PPA	phenylpyruvate
L-MA	L-mandelate
PG	phenylglyoxylate
L-phg	L-phenylglycine
L-glu	L-glutamate
2-OG	2-oxo-glutarate
2-PE	2-phenylethanol
TyrB	aromatic transaminase
PglB/C	pyruvate dehydrogenase
PglA	benzoylformyl-CoA synthetase
PglD	thioesterase
PglE	L-phg amino transferase
HmaS	4-hydroxymandelate synthase
Hmo	4-hydroxymandelate oxidase
HpgAT	4-hydroxyphenylglycine amino transferase
DAT	D-phenylglycine amino transferase
MR	mandelate racemase
MD	S-mandelate dehydrogenase
LeuDH	leucine dehydrogenase
GDH	glutamate dehydrogenase

References

[1] Lu Y, Freeland S. On the evolution of the standard amino-acid alphabet. Genome Biol 2006;7(1):1–6.
[2] Moosmann D, Mokeev V, Kulik A, Osipenkov N, Kocadinc S, Ort-Winklbauer R, Handel F, Hennrich O, Youn JW, Sprenger GA, Mast Y. Genetic engineering approaches for the fermentative production of phenylglycines. Appl Microbiol Biotechnol 2020;104(1):3433–44.
[3] Hönig M, Sondermann P, Turner NJ, Carreira EM. Enantioselective chemo- and biocatalysis: partners in retrosynthesis. Angew Chem Int Ed 2017;56(31):8942–73.
[4] Osipenkov N, Kulik A, Mast Y. Characterization of the phenylglycine aminotransferase PglE from *Streptomyces pristinaespiralis*. J Biotechnol 2018;278(1):34–8.
[5] Ningsih F, Kitani S, Fukushima E, Nihira T. VisG is essential for biosynthesis of virginiamycin S, a streptogramin type B antibiotic, as a provider of the nonproteinogenic amino acid phenylglycine. Microbiol-Sgm 2011;157(1):3213–20.
[6] Liu SP, Liu RX, El-Rotail AAMM, Ding ZY, Gu ZH, Zhang L, Shi GY. Heterologous pathway for the production of L-phenylglycine from glucose by *E. coli*. J Biotechnol 2014;186(1):91–7.
[7] Liu Q, Zhou J, Yang T, Zhang X, Xu M, Rao Z. Efficient biosynthesis of l-phenylglycine by an engineered *Escherichia coli* with a tunable multi-enzyme-coordinate expression system. Appl Microbiol Biotechnol 2018;102(5):2129–41.
[8] Liu SP, Liu RX, Mao J, Zhang L, Ding ZY, Gu ZH, Shi GY. Structural-based screening of L-phenylglycine aminotransferase using L-phenylalanine as the optimal amino donor: recycling of L-phenylalanine to produce L-phenylglycine. Biotechnol Bioproc E 2016;21(1):153–9.
[9] Muller U, van Assema F, Gunsior M, Orf S, Kremer S, Schipper D, Wagemans A, Townsend CA, Sonke T, Bovenberg R, Wubbolts M. Metabolic engineering of the *E. coli* L-phenylalanine pathway for the production of D-phenylglycine (D-Phg). Metab Eng 2006;8(3):196–208.
[10] Tang CD, Shi HL, Jia YY, Li X, Wang LF, Xu JH, Yao LG, Kan YC. High level and enantioselective production of L-phenylglycine from racemic mandelic acid by engineered *Escherichia coli* using response surface methodology. Enzym Microb Technol 2020;136(1):1–12.
[11] Mast YJ, Wohlleben W, Schinko E. Identification and functional characterization of phenylglycine biosynthetic genes involved in pristinamycin biosynthesis in *Streptomyces pristinaespiralis*. J Biotechnol 2011;155(1):63–7.
[12] Hubbard BK, Thomas MG, Walsh CT. Biosynthesis of L-p-hydroxyphenylglycine, a non-proteinogenic amino acid constituent of peptide antibiotics. Chem Biol 2000;7(12):931–42.
[13] Hojati Z, Milne C, Harvey B, Gordon L, Borg M, Flett F, Wilkinson B, Sidebottom PJ, Rudd BAM, Hayes MA, Smith CP, Micklefield J. Structure, biosynthetic origin, and engineered biosynthesis of calcium-dependent antibiotics from *Streptomyces coelicolor*. Chem Biol 2002;9(11):1175–87.
[14] Jariyachawalid K, Laowanapiban P, Meevootisom V, Wiyakrutta S. Effective enhancement of *Pseudomonas stutzeri* D-phenylglycine aminotransferase functional expression in Pichia pastoris by co-expressing *Escherichia coli* GroEL-GroES. Microb Cell Factories 2012;11(1):1–13.
[15] Zhou Y, Wu SK, Li Z. One-pot enantioselective synthesis of D-phenylglycines from racemic mandelic acids, styrenes, or biobased L-phenylalanine via cascade biocatalysis. Adv Synth Catal 2017;359(24):4305–16.
[16] Fan CW, Xu GC, Ma BD, Bai YP, Zhang J, Xu JH. A novel D-mandelate dehydrogenase used in three-enzyme cascade reaction for highly efficient synthesis of non-natural chiral amino acids. J Biotechnol 2015;195(1):67–71.
[17] Cheng J, Xu G, Han R, Dong J, Ni Y. Efficient access to L-phenylglycine using a newly identified amino acid dehydrogenase from *Bacillus clausii*. RSC Adv 2016;6(84):80557–63.
[18] Kratzer R, Woodley JM, Nidetzky B. Rules for biocatalyst and reaction engineering to implement effective, NAD(P)H-dependent, whole cell bioreductions. Biotechnol Adv 2015;33(8):1641–52.
[19] Hwang JY, Park J, Seo JH, Cha M, Cho BK, Kim J, Kim BG. Simultaneous synthesis of 2-phenylethanol and L-homophenylalanine using aromatic transaminase with yeast Ehrlich pathway. Biotechnol Bioeng 2009;102(5):1323–9.
[20] Madje K, Schmolzer K, Nidetzky B, Kratzer R. Host cell and expression engineering for development of an *E. coli* ketoreductase catalyst: enhancement of formate dehydrogenase activity for regeneration of NADH. Microb Cell Factories 2012;11(1):1–8.
[21] Wang P, Yang X, Lin B, Huang J, Tao Y. Cofactor self-sufficient whole-cell biocatalysts for the production of 2-phenylethanol. Metab Eng 2017;44(1):143–9.
[22] Hayashi H, Inoue K, Nagata T, Kuramitsu S, Kagamiyama H. Escherichia coli aromatic amino acid aminotransferase: characterization and comparison with aspartate aminotransferase. Biochemistry-Us 1993;32(45):12229–39.
[23] Challis GL, Hopwood DA. Synergy and contingency as driving forces for the evolution of multiple secondary metabolite production by *Streptomyces* species. P Natl Acad Sci USA 2003;100:14555–61.
[24] Padma PN, Rao AB, Yadav JS, Reddy G. Optimization of fermentation conditions for production of glycopeptide antibiotic vancomycin by *Amycolatopsis orientalis*. Appl Microbiol Biotechnol 2002;102–103(1–6):395–405.
[25] Land M, Lapidus A, Mayilraj S, Chen F, Copeland A, Del Rio TG, Nolan M, Lucas S, Tice H, Cheng JF, Chertkov O, Bruce D, Goodwin L, Pitluck S, Rohde M, Goker M, Pati A, Ivanova N, Mavromatis K, Chen A, Palaniappan K, Hauser L, Chang YJ, Jeffries CC, Brettin T, Detter JC, Han C, Chain P, Tindall BJ, Bristow J, Eisen JA, Markowitz V, Hugenholtz P, Kyrpides NC, Klenk HP. Complete genome sequence of *Actinosynnema mirum* type strain (101). Stand in Genomic Sciences 2009;1(1):46–53.
[26] Hifnawy MS, Fouda MM, Sayed AM, Mohammed R, Hassan HM, AbouZid SF, Rateb ME, Keller A, Adamek M, Ziemert N, Abdelmohsen UR. The genus *Micromonospora* as a model microorganism for bioactive natural product discovery. RSC Adv 2020;10(35):20939–59.
[27] Li MH, Meng XM, Sun ZY, Zhu CJ, Ji HY. Effects of NADH availability on 3-phenyllactic acid production by *Lactobacillus plantarum* expressing formate dehydrogenase. Curr Microbiol 2019;76(6):706–12.
[28] Binay B, Alagoz D, Yildirim D, Celik A, Tukel SS. Highly stable and reusable immobilized formate dehydrogenases: promising biocatalysts for in situ regeneration of NADH. Beilstein J Org Chem 2016;12:271–7.
[29] Khan MIH, Ito K, Kim H, Ashida H, Ishikawa T, Shibata H, Sawa Y. Molecular properties and enhancement of thermostability by random mutagenesis of glutamate dehydrogenase from Bacillus subtilis. Biosci Biotechnol Biochem 2005;69(10):1861–70.
[30] Chen R, Chen Q, Kim H, Siu KH, Sun Q, Tsai SL, Chen W. Biomolecular scaffolds for enhanced signaling and catalytic efficiency. Curr Opin Biotechnol 2014;28(1):59–68.
[31] Qiu XY, Xie SS, Min L, Wu XM, Zhu LY, Zhu LY. Spatial organization of enzymes to enhance synthetic pathways in microbial chassis: a systematic review. Microb Cell Factories 2018;17.
[32] Dueber JE, Wu GC, Malmirchegini GR, Moon TS, Petzold CJ, Ullal AV, Prather KLJ, Keasling JD. Synthetic protein scaffolds provide modular control over metabolic flux. Nat Biotechnol 2009;27(8). 753-U107.
[33] Zhao Y, Feng R, Zheng G, Tian J, Ruan L, Ge M, Jiang W, Lu Y. Involvement of the TetR-type regulator PaaR in the regulation of pristinamycin I biosynthesis through an effect on precursor supply in *Streptomyces pristinaespiralis*. J Bacteriol 2015;197(12):2062–71.
[34] Croteau R, Ketchum RE, Long RM, Kaspera R, Wildung MR. Taxol biosynthesis and molecular genetics. Phytochemistry Rev 2006;5(1):75–97.
[35] van der Meijden MW, Leeman M, Gelens E, Noorduin WL, Meekes H, van Enckevort WJP, Kaptein B, Vlieg E, Kellogg RM. Attrition-enhanced deracemization in the synthesis of clopidogrel - a practical application of a new discovery. Org Process Res Dev 2009;13(6):1195–8.

[36] Wang M, Wu L, Wang L, Xin X. Down-regulation of Notch1 by gamma-secretase inhibition contributes to cell growth inhibition and apoptosis in ovarian cancer cells A2780. Biochem Bioph Res Co 2010;393(1):144–9.
[37] Wei GZ, Bai LQ, Yang T, Ma JA, Zeng Y, Shen YM, Zhao PJ. A new antitumour ansamitocin from *Actinosynnema pretiosum*. Nat Prod Res 2010;24(12):1146–50.
[38] Asamizu S, Abugreen M, Mahmud T. Comparative metabolomic analysis of an alternative biosynthetic pathway to pseudosugars in *Actinosynnema mirum* DSM 43827. Chembiochem 2013;14(13):1548–51.
[39] Watanabe K, Okuda T, Yokose K, Furumai T, Maruyama HB. *Actinosynnema mirum*, a new producer of nocardicin antibiotics. J Antibiot 1983;36(3):321–4.
[40] Davidsen JM, Bartley DM, Townsend CA. Non-ribosomal propeptide precursor in nocardicin A biosynthesis predicted from adenylation domain specificity dependent on the MbtH family protein Nocl. J Am Chem Soc 2013;135(5):1749–59.
[41] Reifenrath M, Boles E. Engineering of hydroxymandelate synthases and the aromatic amino acid pathway enables de novo biosynthesis of mandelic and 4-hydroxymandelic acid with *Saccharomyces cerevisiae*. Metab Eng 2018;45(1):246–54.
[42] Zhang YH, Wang YL, Wang SZ, Fang BS. Engineering bi-functional enzyme complex of formate dehydrogenase and leucine dehydrogenase by peptide linker mediated fusion for accelerating cofactor regeneration. Eng Life Sci 2017;17(9):989–96.
[43] Kashiwagi FM, Ojima Y, Taya M. Metabolic engineering of *Escherichia coli* KO11 with the NADH regeneration system for enhancing ethanol production. J Chem Eng Jpn 2018;51(3):264–8.
[44] Zhu YB, Jiang ZY, Chen JH, Xu JM, Wang LM, Qi B. Fusion of D-lactate dehydrogenase and formate dehydrogenase for increasing production of (R)-3-Phenyllactic acid in recombinant *Escherichia coli* BL21 (DE3). J Biobased Mater Bioenergy 2017;11(4):372–8.
[45] Zhao HM, van der Donk WA. Regeneration of cofactors for use in biocatallysis. Curr Opin Biotechnol 2003;14(6):583–9.
[46] Pham VD, Lee SH, Park SJ, Hong SH. Production of gamma-aminobutyric acid from glucose by introduction of synthetic scaffolds between isocitrate dehydrogenase, glutamate synthase and glutamate decarboxylase in recombinant *Escherichia coli*. J Biotechnol 2015;207(1):52–7.
[47] Tippmann S, Anfelt J, David F, Rand JM, Siewers V, Uhlen M, Nielsen J, Hudson EP. Affibody scaffolds improve sesquiterpene production in Saccharomyces cerevisiae. ACS Synth Biol 2017;6(1):19–28.
[48] Wang YC, Yu O. Synthetic scaffolds increased resveratrol biosynthesis in engineered yeast cells. J Biotechnol 2012;157(1):258–60.
[49] Studier FW. Protein production by auto-induction in high-density shaking cultures. Protein Expr Purif 2005;41(1):207–34.